Polar Biol (2016) 39:1841–1857
DOI 10.1007/s00300-016-1955-5

ORIGINAL PAPER

Late winter-to-summer change in ocean acidification state in Kongsfjorden, with implications for calcifying organisms

A. Fransson[1] · M. Chierici[2] · H. Hop[1,3] · H. S. Findlay[4] · S. Kristiansen[3] · A. Wold[1]

Received: 4 January 2016 / Revised: 10 April 2016 / Accepted: 26 April 2016 / Published online: 5 May 2016

Abstract Late winter-to-summer changes (April to July) in ocean acidification state, calcium carbonate ($CaCO_3$) saturation for aragonite (Ω_a) and calcite (Ω_c) and biogeochemical properties were investigated in 2013 and 2014 in Kongsfjorden, Svalbard. We investigated physical (salinity, temperature) and chemical (carbonate system, nutrient) properties in the water column from the glacier front in the fjord to the west Spitsbergen shelf. The average range of Ω_a in the upper 50 m in the fjord in winter was 1.59–1.74 and in summer 1.65–2.66. The lowest Ω_a (1.5) was close to the reported critical threshold for aragonite-forming organisms such as the pteropod *Limacina helicina*. In summer 2013, Ω_a, pH_T and salinity were generally lower than in 2014 as a result of a larger influence of high-CO_2 water from the coastal current and less Atlantic water. The inner fjord was influenced by glacial water in summer which decreased Ω_a by 0.7. Biological CO_2 consumption based on a winter-to summer decrease in nitrate was larger in 2014 than in 2013, suggesting more primary production in 2014. The influence of freshwater decreased Ω_a by the same amount as the biological effect increased Ω_a. The seasonal increase in temperature only played a minor role on the increase of Ω_a. The biological effect showed more inter-annual variability than the effect of freshwater. Based on this study, we suggest that changes in the inflow of different water masses and freshwater directly influence ocean acidification state, but also indirectly affect the biological drivers of carbonate chemistry in the fjord.

Keywords Carbonate system · Fjord chemistry · Glacier–ocean interaction · Land–ocean interaction · Primary production · Svalbard · Aragonite · Pteropods

Introduction

Specific biogeochemical processes in the Arctic Ocean such as sea-ice formation and meltwater affect the seawater calcium carbonate ($CaCO_3$) saturation state (Ω) and carbonate chemistry during an annual cycle (Chierici et al. 2011). In winter, low Ω has been observed under the sea ice in the Arctic Ocean as an effect of sea-ice dynamics, upwelling of CO_2-rich subsurface waters and remineralization of organic material (Chierici et al. 2011; Shadwick et al. 2011; Fransson et al. 2013). During ice formation and melting in spring, CO_2-rich brine is drained from the sea ice to the water beneath the ice through brine channels, decreasing Ω and pH (e.g., Rysgaard et al. 2007; Fransson et al. 2013). Sea-ice meltwater causes low pH and undersaturated Ω with regard to aragonite in the Arctic Ocean (Chierici and Fransson 2009; Yamamoto-Kawai et al. 2009). The same processes that result in low pH and low carbonate ion concentrations in the Arctic Ocean also affect Arctic fjords. Freshwater supply from glacial drainage water has been shown to affect the carbonate chemistry in Arctic fjords (Sejr et al. 2011;

This article belongs to the special issue on the "Kongsfjorden ecosystem—new views after more than a decade of research," coordinated by Christian Wiencke and Haakon Hop.

✉ A. Fransson
agneta.fransson@npolar.no

[1] Norwegian Polar Institute, Fram Centre, 9296 Tromsø, Norway

[2] Institute of Marine Research, Box 6404, 9294 Tromsø, Norway

[3] Department of Arctic and Marine Biology, UiT The Arctic University of Norway, 9037 Tromsø, Norway

[4] Plymouth Marine Laboratory, Prospect Place, Plymouth, Devon PL1 3DH, UK

Fransson et al. 2015) causing a decrease in Ω with increased freshwater supply, particularly during winter (Fransson et al. 2015). Fjords with tidal glaciers, such as Kongsfjorden, Spitsbergen, are affected by plumes of glacial meltwater and subglacial melt at the glacier front, which induces upwelling of relatively fresh water to the surface or near surface (e.g., Svendsen et al. 2002; Lydersen et al. 2014). The upwelled fresh water supplies the surface waters with nutrients which may increase primary production (if light is not limited by high concentrations of sediments in the surface water) and produce favorable feeding conditions for seabirds and sea mammals (Apollonio 1973; Lydersen et al. 2014). Decreased fugacity of CO_2 (fCO_2) and increases in Ω due to primary production (i.e., biological carbon uptake) have been observed in summer near glacier fronts in Arctic fjords (Sejr et al. 2011; Fransson et al. 2015).

The Ω is used as a chemical indicator for the dissolution potential for solid $CaCO_3$ and consequently for ocean acidification (OA) state. When $\Omega < 1$, solid $CaCO_3$ is chemically unstable and prone to dissolution (i.e., the waters are undersaturated with respect to the $CaCO_3$ mineral). $CaCO_3$ occurs in several solid forms including aragonite (a) and calcite (c) where aragonite is less stable than calcite. Marine biogenic $CaCO_3$, such as shells and skeletons of marine organisms, is biologically formed using a variety of mechanisms involving bicarbonate (HCO_3^-), carbonate ion (CO_3^{2-}) and CO_2 (Findlay et al. 2011). The dissolution of $CaCO_3$ is controlled by the concentrations of CO_3^{2-} and calcium (Ca^{2+}) in the water. In ocean acidification field studies, Ω is thus an indicator for a chemical change in the $CaCO_3$ dissolution potential, but is not always directly related to the biological consequences of ocean acidification. Recent studies on calcifying organisms, in particularly aragonite-forming organisms, have found clear indications for linkages between Ω_a and the integrity of the $CaCO_3$ structures of these organisms under future ocean acidification conditions. The free-swimming pelagic pteropod mollusk *Limacina helicina* is one of few marine organisms (taxa) that produce aragonite shells instead of calcite shells (e.g., Fabry et al. 2008; Bednaršek et al. 2012). This species has been shown to have difficulty in regulating the carbonate chemistry in their internal calcifying fluid at $\Omega < 1.4$, and consequently, they are more sensitive to ocean acidification than other calcifying organisms (Ries 2012; Bednaršek et al. 2014). Comeau et al. (2009, 2010) found in perturbation experiments with *L. helicina* that decreased aragonite precipitation rate highly correlated with low Ω_a and low [CO_3^{2-}] and that shell formation decreased by 28 % at high CO_2 levels (>900 µatm) and at higher temperature (at 4 °C). In addition, Bednaršek et al. (2012, 2014) and Bednaršek and Ohman (2015) found that shell dissolution and thinning of shells in living aragonite-forming pteropods (including *L. helicina*) were strongly related to the Ω_a in the California upwelling zone (naturally low Ω and high fCO_2 due to upwelling along the coast) and in the Scotia Sea, Antarctica. Their studies showed that severe shell dissolution of aragonite-forming organisms, such as *L. helicina*, takes place when $\Omega_a < 1.4$, and substantial thinning of shells occurs at $\Omega_a < 1.2$ (Bednaršek and Ohman 2015).

Regarding their ecological significance, pteropods act as important prey for larger zooplankton as well as salmon (*Salmo salar*), polar cod (*Boreogadus saida*), seabirds and baleen whales (e.g., Gilmer and Harbison 1991; Falk-Petersen et al. 2001; Hunt et al. 2008). In the view of the global carbon budget, the main importance of the pteropods and their aragonite shells is through the transfer of inorganic carbon into the deep ocean (Tréguer et al. 2013; Bauerfeind et al. 2014) and organic carbon export as sinking particles and fecal pellets (Accornero et al. 2003; Manno et al. 2010).

The pteropod *L. helicina*, which is ubiquitous throughout the Arctic Ocean and shelf areas including Spitsbergen fjords, is often located in swarms in surface waters (0–50 m) in spring and summer (Kobayashi 1974; Gannefors et al. 2005). During a 24-h cycle, they migrate from surface to deeper water layers down to >200 m, especially during the night, likely to avoid predators (Comeau et al. 2010; Lischka and Riebesell 2012). In Kongsfjorden, *L. helicina* has a 1-year life cycle (Lischka et al. 2011) and overwinters at depths below 200 m (Gannefors et al. 2005; Lischka et al. 2011). They become adults in early summer and reproduce in July/August and their veligers grow and become juveniles in autumn (Lischka et al. 2011). The juveniles also overwinter at depths below 200 m and continue to grow in spring to become adults in early summer (Gannefors et al. 2005; Lischka and Riebesell 2012). Most studies confirm that early stages of *L. helicina* are the most vulnerable (e.g., Kurihara 2008; Comeau et al. 2010; Lischka et al. 2011) since they have not fully developed with shells (Kobayashi 1974; Fabry et al. 2008). In the Canadian Arctic, a seasonal study of the carbonate system during a full annual cycle showed that the surface layer had the largest Ω_a variation and that the water below 50 m had $\Omega_a < 1$ from November to April (Chierici et al. 2011). The study also showed dramatic decreases in Ω_a during autumn and winter as a result of increased CO_2 due to physical mixing of CO_2-rich subsurface waters, sea-ice dynamics producing CO_2-rich brine and respiration of organic of matter (Chierici et al. 2011; Fransson et al. 2013). Despite these conditions, the juvenile *L. helicina* is presently able to persist this sensitive period of their life cycle at low food availability, although they do appear to have limited growth at this time. Indeed, there is evidence that *L. helicina* (and *L. retroversa*) cease growth in winter (Lischka and Riebesell 2012). Some organisms can survive low food periods such as winter on stored lipids. Gannefors et al. (2005) found two to three times more lipids (stored lipids and membrane

lipids) in veligers and juveniles than in adult female *L. helicina*. However, it is unclear whether *L. helicina* lives on stored lipids during winter. For example, lipids found in juvenile *L. helicina* in Kongsfjorden in May could have been accumulated and stored before overwintering or equally could have been fresh lipids accumulated in April/May with the onset of the spring bloom (Gannefors et al. 2005). The ability to feed or utilize energy (lipid) stores over winter is important for organisms to cope with environmental stressors such as low Ω_a. Hence, the winter period is likely to be the most challenging for *L. helicina* with regard to low Ω_a levels, as ocean acidification continues to alter carbonate chemistry in the future.

The inner parts of Kongsfjorden are comparable to Arctic conditions due to cold local, winter cooled water and fresh surface water from glacial meltwater (and river supply), while the outer parts are influenced by the warm and saline Atlantic water (or transformed Atlantic water; Hop et al. 2006). These conditions result in physical and chemical gradients that make Kongsfjorden a suitable natural laboratory to investigate impacts of different stressors, such as ocean acidification on calcifying organisms. Several studies in Kongsfjorden have focused on the physical and biological properties, but few studies have described the carbonate chemistry and Ω and ocean acidification state. Hence, in this paper, we (1) present seasonal and inter-annual variability in hydrography (salinity, temperature), carbonate chemistry (pH, fCO_2, Ω) and nutrients from late winter (April) and summer (July) 2013 and 2014 and discuss the implication for calcifying marine organisms; (2) investigate the effect of freshwater supply (e.g., glacial drainage water, Arctic regime) and Atlantic water inflow on the OA state and Ω from the glacier front to the shelf/adjacent water; and (3) compare the seasonal signal in Ω in two contrasting regimes, Arctic and Atlantic, and discuss the effect of increased Atlantic water inflow and increased freshwater runoff, with possible consequences for calcifying (e.g., aragonite-forming) organisms.

Study area

Kongsfjorden is situated on western Spitsbergen and is oriented from southeast to northwest between 78°50′ and 79°04′N and 11°20′ and 12°30′E (Fig. 1). The entire fjord is 20 km long and has no pronounced sill (Svendsen et al. 2002). However, the inner fjord basin, which is <100 m deep, has a sill of about 20 m (Hop et al. 2002). Further out, the fjord is deeper (>300 m) and more influenced by Atlantic water (e.g., Cottier et al. 2005, 2007; Hop et al. 2006). The fjord has two tidal glaciers (Kronebreen and Kongsbreen) at the inner part of the fjord, where the depth near the glacier front is shallow (60–90 m). It has typical fjord circulation where the water masses in fjord consist of three to five layers: a fresh surface layer in summer (SW), a layer of intermediate water (IW), transformed Atlantic water (TAW) in the middle to outer part and local fjord water (LW) in the deeper part of the fjord, including winter cooled water (WCW) mainly in the inner bay (Hop et al. 2006). The TAW is dominated by Atlantic water (AW), which has its origin in the West Spitsbergen Current (WSC) and is mixed with Arctic water (ArW) on the shelf when it is advected into Kongsfjorden (Cottier et al. 2005). The waters transported in the coastal current (CC) on the western side of Spitsbergen originate from the area east of Spitsbergen and has lower salinity and is colder than WSC (Walczowski 2013). This water rounds the southern Cape of Svalbard (Sørkapp) and is sometimes referred to as the Southern Cape Current before it reaches the western shelf (blue arrows, in Fig. 1). The SW is affected by warming, freshening and biological processes in summer, and in winter, the upper layer is mainly affected by sea-ice dynamics and cooling. The cold and saline WCW is formed during winter as a result of cooling, sea-ice formation and the sinking of dense cooled water (Svendsen et al. 2002). Landfast fjord ice forms in autumn and winter (Gerland and Renner 2007) although recently the distribution of the fast ice has declined, with less sea ice after 2006. Fast ice is now generally limited to the inner bay, with least ice recorded in 2012 (S. Gerland, Norwegian Polar Institute, unpubl. data). In spring (May/early June), the sea ice melts and contributes to the stratification of the surface water (Svendsen et al. 2002). In the fjord, there is large inter-annual variability in temperature with warm periods in 2006–2008 and 2012–2013 (Dalpadado et al. 2016). The fjord is largely affected by meltwater discharge, up to 45 km distance from the glacier front (i.e., >10 km outside the fjord) and up to 30 m depth in the inner part (Keck et al. 1999; Hop et al. 2002, 2006; Svendsen et al. 2002), which results in strong surface stratification during summer. As an effect of increased WSC, the fjord water is expected to become warmer resulting in larger discharge of meltwater into Kongsfjorden (Piquet et al. 2014). Primary production starts in spring, between April and May, with the highest chlorophyll *a* in the inner parts of the fjord (Hodal et al. 2012; Hegseth and Tverberg 2013). However, in July the chlorophyll *a* near the glacier front is insignificant due to supply of sediments causing light limitation (Lydersen et al. 2014).

Materials and methods

The summer data were collected in July 2013 and 2014 with R/V *Lance* as part of the Kongsfjorden pelagic survey (as part of Monitoring of Svalbard and Jan Mayen Kongsfjorden survey, MOSJ). In late winter (April 2013 and 2014), water was sampled from the surface water from

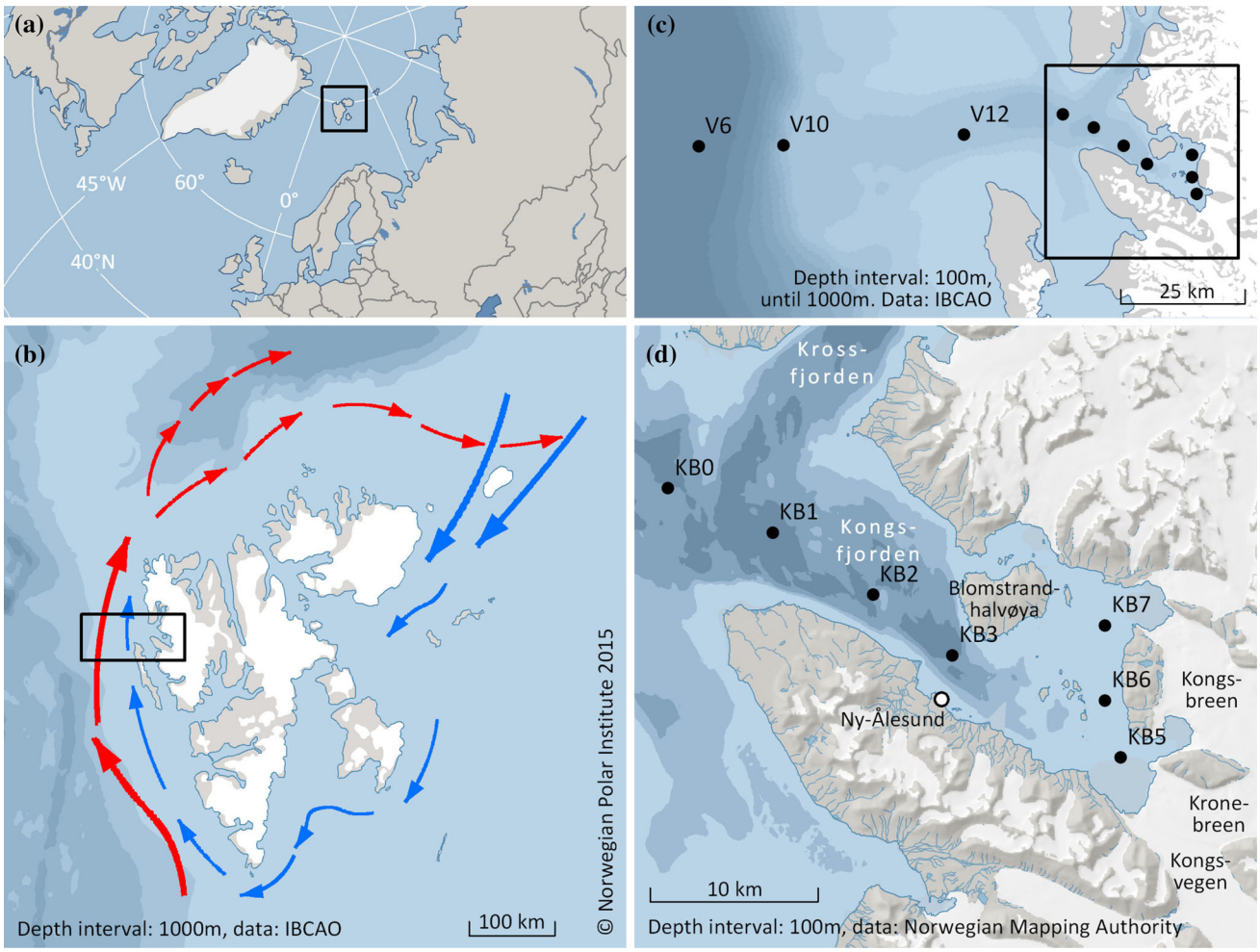

Fig. 1 Map of **a** Svalbard location, **b** surface currents around Svalbard showing the cold and relatively fresh Arctic water transported by the East Spitsbergen Current, also referred to as the coastal current west of Spitsbergen (CC, *blue arrows*), and the warm and saline Atlantic water (AW, *red arrows*) transported in the West Spitsbergen Current (WSC). Bathymetry on the maps is shown in *different shades of blue* representing the depth of the contour in meters, with greater depths in *darker blue*. *White areas* on land are glaciers, and SC denotes the South Cape (no: Sørkapp) **c** sampling stations (*black dots*) in Kongsfjorden (*area in black box*) and on the adjacent shelf (V6, V10 and V12), **d** station location (*black dots*) and station numbers from the glacier fronts of Kongsbreen (Kb6 and Kb7) and Kronebreen (Kb5) to the mouth of the Kongsfjorden (Kb0). (Color figure online)

small boats supplied by the Sverdrup station and Kings Bay in Ny-Ålesund in the inner part of the fjord. In July onboard R/V *Lance*, water was sampled from Niskin bottles mounted on a rosette with conductivity–temperature–pressure sensors (Seabird SBE 911 CTD). Temperatures of the winter water column samples were measured on site, immediately after the sample recovery, using a digital probe (Testo 720) with the precision of ±0.1 °C and accuracy of ±0.1 °C. Salinity of discrete samples was measured by a conductivity meter (WTW Cond 330i, Germany) with the precision and accuracy of ±0.05. In addition to sample-bottle measurements of temperature and salinity, we obtained hydrography data by deploying CTD probes on the stations (Table 1). In April 2013, we used a SBE 37 MicroCAT (Seabird Electronics, USA) with a salinity resolution of ±0.0001 and accuracy of ±0.003 and temperature resolution of 0.0001 °C and accuracy of 0.002 °C onboard the *Polarcirkel*. In April 2014 we used a CTD SD204 (SAIV A/S, Norway) with a salinity resolution of ±0.01 and accuracy of ±0.02 and a temperature resolution of 0.001 °C and accuracy of ±0.01 °C onboard the MV *Teisten*. Water for the carbonate system was sampled directly into 250-mL borosilicate bottles and immediately preserved with saturated mercuric chloride ($HgCl_2$; 60 µL to 250 mL sample) and stored dark at 4 °C. The sampling from the small boat and from the sea-ice edge in April 2013 and 2014 was done with a polyethylene water sampler, immersed directly into the water column, where there was no sea ice. We transferred the water to 1-L bottles (Nalgene®, Rochester, NY, USA), and immediately after return

Table 1 Summary of the sampling dates, stations, locations in the fjord (GF = glacier front, MF = mid-fjord and OF = outerfjord, SH = shelf, OSH = outer shelf), position (see also Fig. 1), bottom depth (m) and number of water samples for each station (*n*) during 2014 and 2013

Sampling date	Station	Location	Latitude (decimal degrees N)	Longitude (decimal degrees E)	Bottom depth (m)	*n*
16.04.2013	KB3	MF	78.95	11.96	329	6
	KB5*	GF	78.90	12.44	68	6
23.07.2013	KB3	MF	78.95	11.96	329	8
	KB5	GF	78.90	12.44	68	5
	V12	OSH	78.98	10.22	217	7
	V10	OSH	78.93	8.54	300	8
	V6	OSH	78.91	7.75	1120	7
25.04.2014	KB7	GF	78.97	12.38	64	5
	KB6	GF	78.93	12.39	83	5
	KB5	GF	78.90	12.44	96	6
	KB3	MF	78.95	11.96	329	8
	KB2	OF	78.98	11.73	330	8
23.07.2014	KB7	GF	78.97	12.38	64	6
	KB6	GF	78.93	12.39	83	6
	KB5	GF	78.90	12.44	96	6
	KB3	MF	78.95	11.96	329	7
	KB2	OF	78.98	11.73	330	7
	KB1	OF	79.01	11.44	352	7
	KB0	SH	79.03	11.14	315	7
24.07.2014	V12	OSH	78.98	9.55	224	6
	V10	OSH	78.97	8.55	300	7
	V6	OSH	78.91	7.77	1120	11

Samples were obtained at the following depths: 0, 5, 10, 25, 50, 100, 200, 300 m, depending on the bottom depth. *Kb5 in April 2013 was sampled on the following depths: 0, 3, 7, 15, 19, 30 m

to the Marine laboratory at Ny-Ålesund, the water samples for the determination of the carbonate system were transferred carefully to 250-mL borosilicate bottles using tubing to prevent contact with air. Samples were preserved with saturated mercuric chloride using the same procedure as onboard RV *Lance*. In parallel to carbonate system sampling, nutrients were sampled in acid-washed 125-mL bottles (Nalgene®, Rochester, NY, USA) and stored dark in freezer at −20 °C during April 2013 and during July 2014, while the nutrients from July 2013 were stored on 20-mL acid-washed vials, then added 200 µL chloroform and stored at 4 °C until analyses. In April 2014, 50 mL of seawater was filtered (GF/F filters) into acid-cleaned, aged, 60-mL bottles (Nalgene®, Rochester, NY, USA). Bottles were stored frozen (−20 °C).

The water samples were analyzed for total alkalinity (A_T), total inorganic carbon (C_T), dissolved inorganic nutrients (nitrate, nitrite, phosphate and silicic acid) and salinity approximately 2 months after the field work. C_T and A_T were analyzed at the Institute of Marine Research (IMR), Tromsø, Norway, following the method described in Dickson et al. (2007). Briefly, C_T was determined using gas extraction of acidified samples followed by coulometric titration and photometric detection using a Versatile Instrument for the Determination of Titration carbonate (VINDTA 3C, Marianda, Germany). The A_T was determined in the water column samples from potentiometric titration with 0.1 N hydrochloric acid using a Versatile Instrument for the Determination of Titration Alkalinity (VINDTA 3C, Marianda). The average standard deviation for C_T and A_T, determined from replicate sample analyses from one sample, was within ±1 µmol kg^{-1}. Routine analyses of Certified Reference Materials (CRM, provided by A. G. Dickson, Scripps Institution of Oceanography, USA) ensured the accuracy of the measurements, which was better than ±1 and ±2 µmol kg^{-1} for C_T and A_T, respectively.

Dissolved inorganic nutrient concentrations of nitrate ($[NO_3^-]$) + nitrite ($[NO_2^-]$), phosphate ($[PO_4^{3-}]$) and silicic acid ($[Si(OH_4)]$) were analyzed at UiT The Arctic University of Norway (April 2013 and July 2014), at the Institute of Marine Research (IMR), Bergen, Norway (July 2013), and the Plymouth Marine Laboratory (PML), UK (April 2014). For the April 2013 and July 2014 nutrients, colorimetric determinations of $[NO_3^-] + [NO_2^-]$ and of

soluble reactive phosphorus and orthosilicic acid were performed in triplicate using a Flow Solution IV analyzer (O.I. Analytical, USA) with routine seawater methods adapted from Grasshoff et al. (2009). The analyzer was calibrated using reference seawater from Ocean Scientific International Ltd. UK, and analytical detection limits (precision) were obtained from six replicate analyses on the same sample. The detection limits were 0.02 mmol m^{-3} for [NO_3^-], 0.01 mmol m^{-3} for [PO_4^{3-}] and 0.07 mmol m^{-3} for [$Si(OH_4)$], respectively. The nutrient samples from 2013 were analyzed at IMR, Bergen, and the following nutrients [NO_2^-], [NO_3^-], [PO_4^{3-}] and [$Si(OH_4)$] were measured spectrophotometrically at 540, 540, 810 and 810 nm, respectively, on a modified Scalar autoanalyser (Bendschneider and Robinson 1952, RFA methodology). The detection limits were 0.06 mmol m^{-3} for [NO_2^-], 0.04 mmol m^{-3} for [NO_3^-], 0.06 mmol m^{-3} for [PO_4^{3-}] and 0.07 mmol m^{-3} for [$Si(OH_4)$]. The nutrient samples from April 2014 analyzed at the PML (Woodward and Rees 2001) used a Bran & Luebbe AAIII segmented flow autoanalyser (SPX Flow Technology Norderstedt, Germany) for the colourimetric determination of inorganic nutrients: combined [NO_3^-] + [NO_2^-] (Brewer and Riley 1965), [NO_2^-] (Grasshoff 1976), [PO_4^{3-}] (Zhang and Chi 2002) and [$Si(OH_4)$] (Kirkwood 1989). Nitrate concentrations were calculated by subtracting the nitrite from the combined [NO_3^-] + [NO_2^-] concentration. The detection limits for [NO_3^-] and [PO_4^{3-}] were 0.02 mmol m^{-3}, [NO_2^-] 0.01 mmol m^{-3}. The accuracy was 1–2 % for all nutrients according to GO-SHIP recommendations.

Calculations

We used C_T, A_T, [PO_4^{3-}], [$Si(OH_4)$], salinity, temperature and depth (pressure) for each sample as input parameters in a CO_2-chemical speciation model (CO2SYS program, Pierrot et al. 2006) to calculate all the other parameters in the carbonate system such as pH, fugacity of CO_2 (fCO_2) and calcium carbonate saturation states in the water column (Ω) for aragonite (Ω_a) and calcite (Ω_c). We used the total hydrogen-ion scale (pH_T), the HSO_4^- dissociation constant from Dickson (1990) and from Mucci (1983) for the solubility products of aragonite and calcite and the carbonate system dissociation constants (K^*1 and K^*2) estimated by Mehrbach et al. (1973) and modified by Dickson and Millero (1987).

The freshwater fractions were calculated using the following Eq. 1:

$$\text{Freshwater fraction} = 1 - S_{MEAS}/S_{REF} \quad (1)$$

where S_{REF} is the mean salinity of the average of winter water salinity in the upper 30 m (WSW) in April 2013 and 2014 (34.83 ± 0.01; $n = 18$), and S_{MEAS} is the measured salinity in the water samples. S_{REF} is within the salinity range (34.7–34.96) of the transformed Atlantic water (TAW) reported by Svendsen et al. (2002). The WSW ($T < 0$ °C) of the inner parts of the fjord (glacier front) also falls within the salinity and temperature ranges of winter cooled water (WCW; $S > 34.4$, $T < -0.5$ °C), whereas the winter water in the middle parts of the fjord is more similar to TAW ($S > 34.7$; $T > 1$ °C; Svendsen et al. 2002). However, we used the salinity and temperature ranges of <34.96 and $T < 0$ °C, respectively, for the mean value of S_{REF}.

Results

Inter-annual and spatial variability of physical and chemical properties in summer 2013 and 2014

Temperature data from July 2013 and 2014 showed a gradual warming from the inner fjord to the shelf (Fig. 2a, b), with the warmest (>7 °C) water found on the outer shelf (V10). The coldest surface water was near the glacier front (Kb5). The fjord water temperature was generally colder in 2013 than in 2014 (Fig. 2a, b). In 2013, the coldest water was found at the bottom parts of the fjord (<1.5 °C) and near the glacier front (0.9 °C), while in 2014 the bottom water in the fjord (>2 °C) and water near the glacier front (>3 °C) were warmer (Fig. 2a, b). In the water layer between 100 and 250 m (2013), the temperature varied spatially, being colder (2–3 °C) inside the fjord and warmer (4 °C) outside the fjord and on the shelf, while in 2014 the temperature was quite homogenous at 3–4 °C throughout the study area.

In both 2013 and 2014 the salinity showed a gradual increase from the inner fjord to the shelf with the most saline water (>35) found on the outer shelf (V10) (Fig. 2c, d). Inside the fjord, the freshest water was found in the upper 30 m near the glacier front (Kb5). Here, the largest variability in salinity was observed, and in 2013, the salinity varied from 31.30 near the glacier front to 34.83 at V10 (Fig. 2c). In 2014, the salinity varied from 31.73 near the glacier front to 35.11 at V10 (Fig. 2d). The salinity was generally lower in the outer parts of the fjord and on the shelf in 2013 than in 2014 (Fig. 2c, d). The highest salinity of >35 in 2013 was limited to the shelf (V6, V10), while in 2014, the high salinity plume reached into the fjord (Kb3; Fig. 2c, d).

Nutrient concentrations showed spatial variability across the study area with the highest values found below 100 m depth on the shelf (i.e., [NO_3^-] > 10 mmol m^{-3}) in both years (Fig. 3a, b). In both 2013 and 2014, high [NO_3^-] was also found at the bottom waters in the fjord although the concentration was lower in 2013 than in 2014 (Fig. 3a, b). The concentration gradients of nutrients (nutriclines)

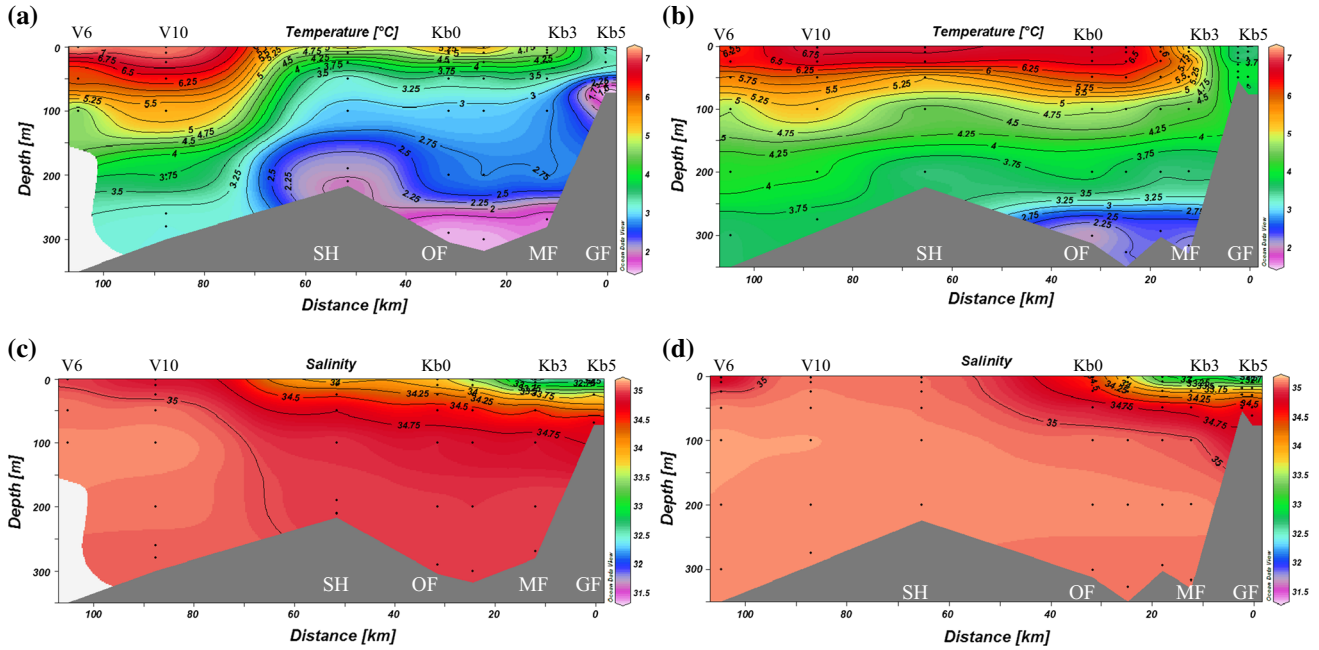

Fig. 2 Section plots of temperature (*T*, °C) and salinity (*S*) in the upper 350 m from the glacier front (distance 0 km) to the fjord mouth (Kb0 ~distance 30 km from front) and to the adjacent shelf (V12 to V6) in July 2013 (**a**, **c**) and in July 2014 (**b**, **d**)

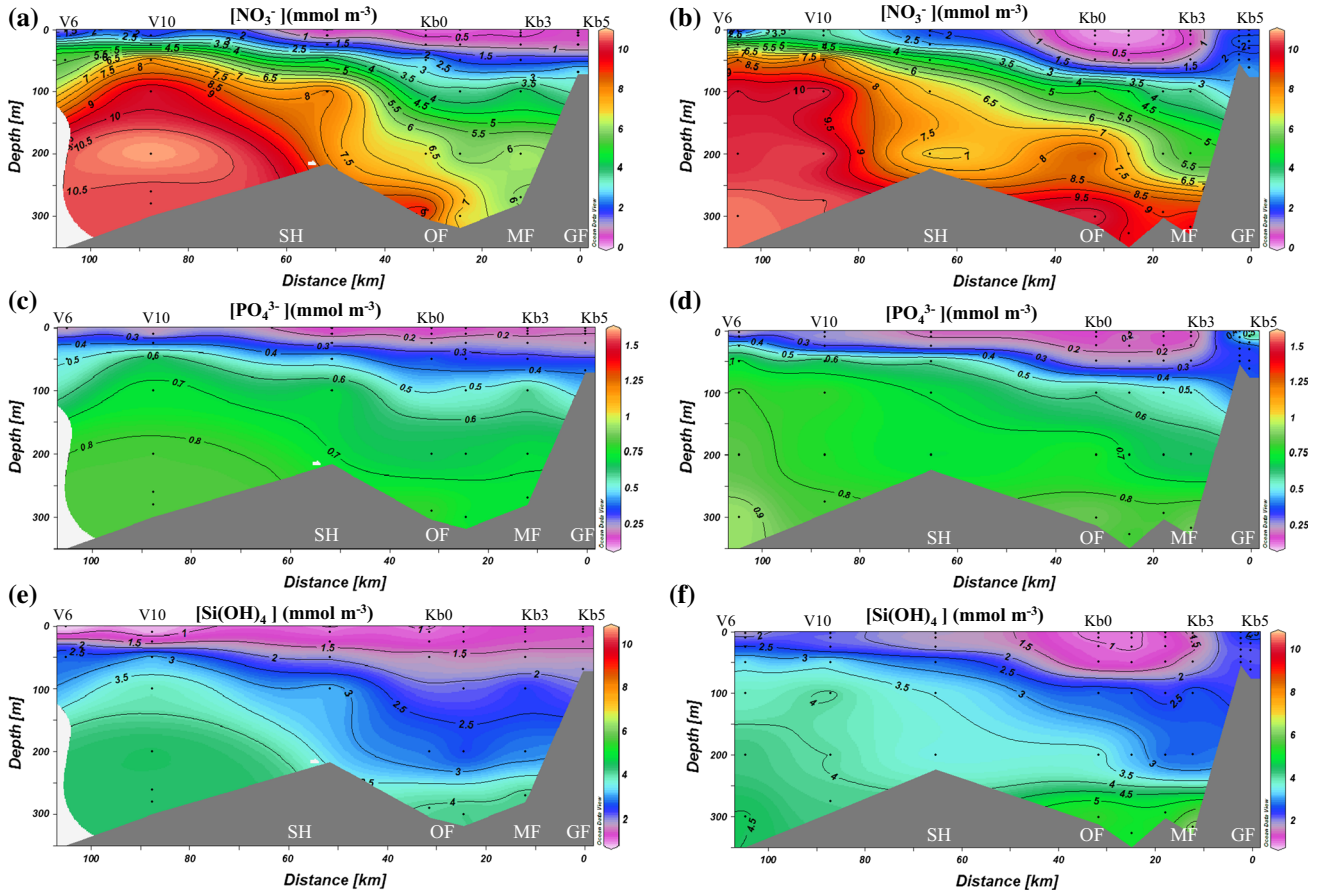

Fig. 3 Section plots of nitrate ($[NO_3^-]$), mmol m^{-3}), phosphate ($[PO_4^{3-}]$), mmol m^{-3}) and silicic acid ($[Si(OH)_4]$, mmol m^{-3}), in the upper 350 m from the glacier front (distance 0 km) to the fjord mouth (Kb0 ~distance 30 km from front) and to the adjacent shelf (V12 to V6) in July 2013 (**a**, **c**, **e**) and in July 2014 (**b**, **d**, **f**)

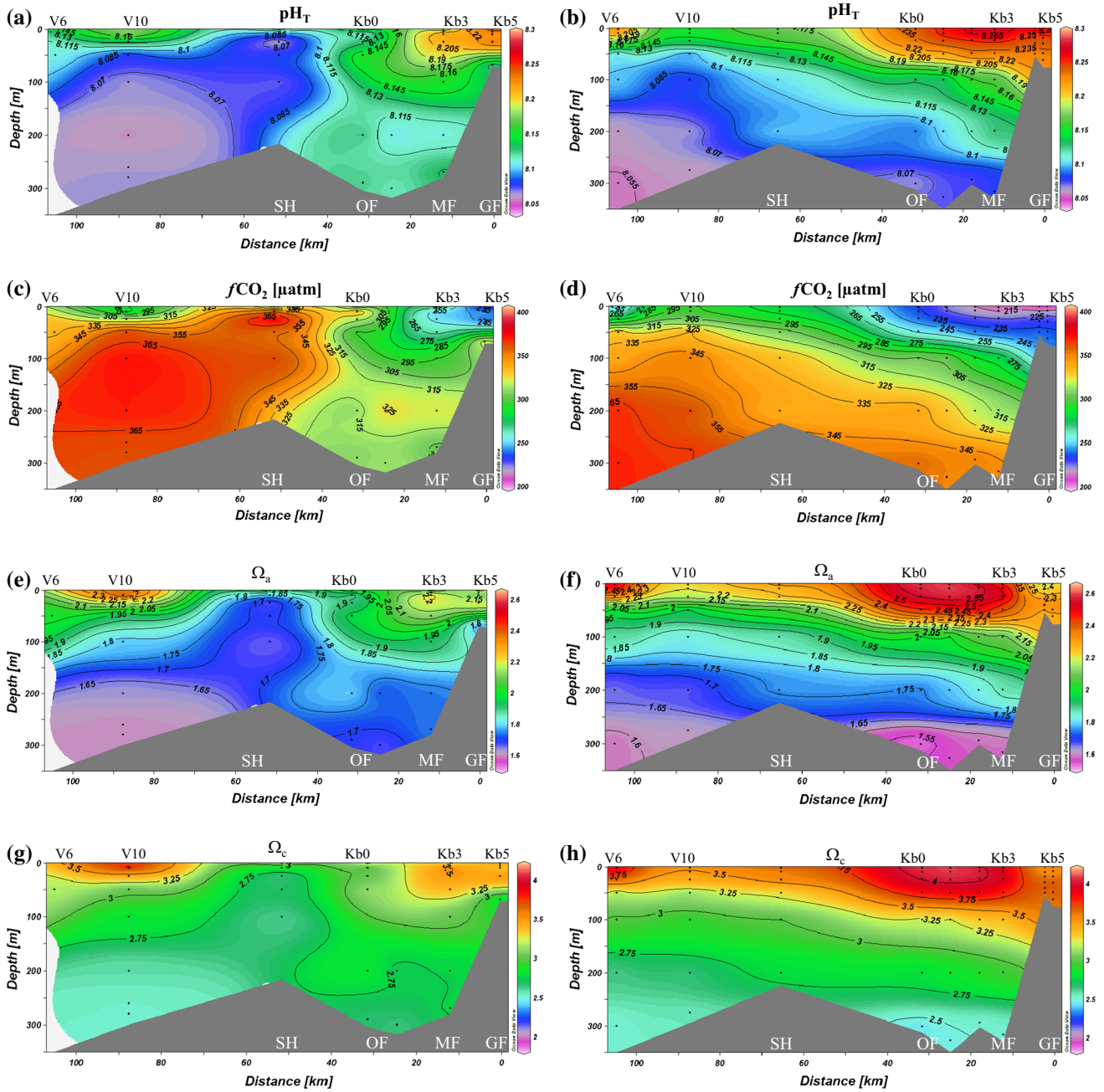

Fig. 4 Section plots of ocean acidification parameters; pH_T, fugacity of carbon dioxide (fCO_2, µatm), aragonite saturation (Ω_a) and calcite saturation (Ω_c) in the upper 350 m from the glacier front (distance 0 km) to the fjord mouth (Kb0 ~distance 30 km from front) and to the adjacent shelf (V12 to V6) in July 2013 (*left side*; **a**, **c**, **e**, **g**) and in July 2014 (*right side*; **b**, **d**, **f**, **h**)

deepened from the shelf toward the fjord and glacier front in both years. For example, [NO_3^-] of 5 mmol m^{-3} was found at 25 m on the shelf slope (V6) and deepened to >150 m in the middle part of the fjord and also extended across a larger depth interval relative to the stations on the slope (Fig. 3a, b). A similar trend was observed for the nutriclines of [PO_4^{3-}] and [$Si(OH_4)$] at 0.6 and 3 mmol m^{-3}, respectively (Fig. 3d–g). For both years the largest variability in [NO_3^-], [PO_4^{3-}] and [$Si(OH_4)$] was in the upper 50 m in the fjord, while concentrations were low or below detection limit in most other parts of the fjord, except for near the glacier front in 2014, where all nutrient concentrations were higher (Fig. 3a–f). Depletion of [NO_3^-] occurred in both years, but was more pronounced and extended deeper in 2014 (Fig. 3a, b).

In 2013, in the upper 50 m of the fjord, pH_T varied from about 8.25 near the glacier front to 8.11 in the outer parts of the fjord (Fig. 4a). In 2014, pH_T showed little spatial

variability with distance from the glacier (Fig. 4b). In general, pH_T in 2013 was lower than in 2014 at the same depth and location (Fig. 4a, b). In 2014, the highest pH_T values (8.28) were recorded mid-fjord (Kb3, Fig. 4b), approximately 10 km from the glacier front. pH_T values decreased from 8.28 in surface to 8.05 at the bottom on the slope (Fig. 4b). In 2013, the highest pH_T was in the upper 50 m near the glacier front, while in the middle and outer parts of the fjord pH_T showed little variability with depth (Fig. 4a) and the lowest pH_T (8.06) was found on the shelf below 200 m. The pH_T values were relatively low (8.13 in 2013 and 8.06 in 2014) in the bottom waters of the outer part (Kb0) of Kongsfjorden in both years.

The surface water fCO_2 showed a gradual increase from the glacier front to the shelf in both years (Fig. 4c, d). fCO_2 was generally higher in 2013 than in 2014 at the same depth and location (Fig. 4c, d). In 2013, surface water fCO_2 ranged from 197 µatm (at 0–2 m) at the glacier front (Kb5) to the highest surface water values of 251 µatm (at 0–2 m, V12, Fig. 4c). In 2014, fCO_2 ranged from 192 µatm (0–2 m) at the glacier front to the highest surface water values of 308 µatm and 274 µatm at V10 and V12, respectively (Fig. 4d). Subsurface waters contained higher fCO_2 than the surface water. In 2013, the highest value of 383 µatm was found below 50 m depth, while in 2014 this value was found below 200 m depth on the slope (V6 and V10, Fig. 4c, d).

In the surface water inside the fjord, the aragonite saturation, Ω_a, was generally lower in 2013 than in 2014 (Fig. 4e, f). At all stations, including the shelf and slope, Ω_a decreased with depth, except in 2014 at the glacier front, where Ω_a was relatively constant with depth. The lowest Ω_a (1.6) in 2013 was found in the deeper parts of the outer shelf (V6) at 250–300 m and in 2014 (1.51) in the bottom water of the outer fjord (Kb0) (Fig. 4a, b). In 2013, low Ω_a was also found at more shallow depths (from 25 m to below 200 m) on the shelf (Fig. 4a). The trend and variability of Ω_c were similar to those for Ω_a, but with higher values (3.5) near the glacier front increasing to $\Omega_c > 4$ (2014) in the outer parts of the fjord and on the slope (V6, Fig. 4h). In 2013, Ω_c decreased from the glacier front to the outer parts of the fjord (Kb0) and then increased again on the slope (V6, V10; Fig. 4g).

Water mass properties in winter and summer

Saline and warm AW was only present in the fjord in 2014, whereas in 2013 the Atlantic influence was classified as TAW (Table 2). AW contained the highest mean A_T of 2319 µmol kg^{-1} with little variability. The TAW was warmer and more saline in 2014 than in 2013. The mean C_T in the TAW was about 60 µmol kg^{-1} higher in 2013 than in 2014. Consequently, pH_T and Ω_a values were lower and fCO_2 was about 75 µatm higher in 2013. In 2013, the mean Ω_a (Ω_c) in the TAW was 1.9 (3.0), which was about 0.5 (0.8) lower than in 2014 ($\Omega_a = 2.4$, $\Omega_c = 3.8$). The highest pH_T of 8.27, Ω_a of 2.5 and Ω_c of 4 were found in the locally formed summer surface water (SSW, upper 50 m) in July 2014. In 2014, Ω_a in the surface water decreased by about 0.8 between summer and winter, which implied a larger seasonal decrease in Ω_a (0.5) than in 2013. Generally, the surface water winter values (WSW) showed little difference between years with regard to salinity, pH_T and $CaCO_3$ saturation values, even though C_T and A_T values were about 10 µmol kg^{-1} lower in April 2014 than in April 2013. The average range of Ω_a in the upper 50 m in the fjord (both years) in winter was 1.59–1.74 and in summer 1.65–2.66.

Late winter-to-summer changes in 2013 and 2014

For the seasonal and inter-annual comparison of physical and chemical properties in two regimes (Atlantic and Arctic), we used data from the upper 30 m in the fjord over the 2 years at two locations (Table 1): the glacier front (Kb5) and at the mid-fjord station (Kb3; Tables 3, 4). In late winter (April), the temperature showed less variability in the upper 30 m than in summer (July) in both 2013 and 2014. Late winter mean temperatures varied between 0.4 °C (2013) and 1.8 °C (2014) at the mid-station and −1.2 °C (2013) and −0.1 °C (2014) at the glacier front station (Kb5). In summer, the temperature ranged between 4.7 °C (2013) and 5.1 °C (2014) at the mid-station and between 3.1 °C (2013) and 3.7 °C (2014) at the glacier front. The seasonal change in temperature was larger in 2013 than in 2014, with the largest seasonal change (4.3 °C) occurring near the glacier front in 2013. In late winter 2013, the upper 30 m was colder than in 2014 (Tables 3, 4).

Salinity was lower in late winter of 2013 than in 2014 at both the mid-station (34.85 in 2013 and 35.13 in 2014) and the glacier front station (34.80 in 2013 and 34.84 in 2014). The salinity was also generally lower in summer than in late winter in both years, with summer salinity of 32.91–32.94 at both mid- and glacier front stations in 2013 and 33.02–33.16 in 2014. The seasonal salinity decrease from April to July in 2013 was 1.90 and 1.98 at the mid-station and glacier front, respectively, while in 2014 the salinity decrease was lowest (1.82) near the glacial front (Tables 3, 4).

In order to compare parameters measured at different salinities, we normalized all parameters to the salinity of 35. The seawater fCO_2 was undersaturated during late winter and summer in both years (Tables 3, 4) with respect to the atmospheric value of about 400 µatm (Zeppelin Observatory, Svalbard, Ny-Ålesund, NILU—Norwegian Institute for Air Research). The fCO_2 values were higher in winter than in summer for both years. The largest seasonal fCO_2 decrease (loss between winter and summer) of about

Table 2 Physical and chemical properties of the water masses in the Kongsfjorden showed as mean, minimum (min) and maximum (max) values in the Atlantic water (AW), transformed Atlantic water (TAW), surface summer water (SSW) and surface winter water (WSW) in 2013 and 2014

Water mass	AW	AW		TAW		TAW		SSW		SSW		WSW		WSW	
Year	2013	2014		2013		2014		2013		2014		2013		2014	
		Mean	Min, max	Mean	Min, max	Mean	Min, max	Mean	Min, max	Mean	Min, max	Mean	Min, max	Mean	Min, max
Salinity	0	35.08	35.00, 35.12	34.81	34.73, 34.89	34.91	34.84, 34.95	33.34	31.22, 34.58	33.25	30.99, 34.65	34.85	34.81, 34.87	34.84	34.80, 34.87
Temp (°C)	0	4.66	3.42, 6.63	3.00	2.85, 3.22	4.72	3.21, 6.69	4.34	2.77, 5.69	5.40	2.72, 6.86	0.45	0.44, 0.47	−0.11	−0.17, −0.02
A_T (μmol kg^{-1})	0	2320	2309, 2327	2316	2306, 2330	2304	2282, 2321	2240	2160, 2308	2239	2156, 2303	2309	2307, 2314	2297	2296, 2299
C_T (μmol kg^{-1})	0	2126	2072, 2157	2141	2104, 2205	2078	2061, 2112	2065	1961, 2176	2001	1939, 2064	2160	2159, 2163	2149	2146, 2154
pH	0	8.148	8.081, 8.246	8.133	8.008, 8.204	8.227	8.205, 8.238	8.181	8.038, 8.291	8.265	8.226, 8.300	8.117	8.107, 8.128	8.126	8.118, 8.135
fCO_2 (μatm)	0	299	231, 350	316	257, 431	242	235, 257	277	197, 396	215	192, 240	321	313, 328	312	305, 317
Ω_c	0	3.24	2.72, 4.07	2.99	2.32, 3.43	3.79	3.49, 4.14	3.28	2.32, 4.01	3.96	3.42, 4.22	2.63	2.57, 2.70	2.61	2.56, 2.66
Ω_a	0	2.05	1.72, 2.57	1.89	1.46, 2.16	2.39	2.20, 2.62	2.06	1.46, 2.53	2.50	2.15, 2.66	1.65	1.62, 1.69	1.64	1.61, 1.67
NO_3 (mmol m^{-3})	0	4.00	0.26, 9.52	3.54	1.89, 5.05	2.36	0.00, 3.10	0.40	0.02, 0.83	0.68	0.00, 2.70	9.95	9.59, 10.27	11.22	7.74, 11.94
PO_4 (mmol m^{-3})	0	0.51	0.20, 0.81	0.49	0.36, 0.68	0.28	0.11, 0.43	0.18	0.09, 0.31	0.30	0.08, 1.61	0.78	0.69, 0.85	0.72	0.61, 0.79
$Si(OH)_4$ (mmol m^{-3})	0	2.37	0.75, 3.82	2.11	1.66, 2.72	1.93	0.85, 2.66	1.19	0.82, 1.59	1.53	0.76, 3.97	4.72	4.53, 4.95	4.74	3.34, 5.07

For inter-annual comparison the values are based on stations from Kb0 to Kb5 and excluded Kb6 and Kb7 since those stations were only collected in 2014. The (–) denotes that AW was not found in 2013 based on the criteria used in this study of $S > 34.96$ and $T > 3$ °C. Aragonite and calcite saturation are denoted Ω_a and Ω_c, respectively

Table 3 Mean values and range shown as the minimum value (min) and the maximum value (max) of chemical and physical properties in winter (w) and summer (s) in the upper 30 m at two station locations in Kongsfjorden (mid, Kb3) and at the glacier front (GF, Kb5) in 2013

Year	2013		2013		2013	2013		2013		2013
Station	Kb3w		Kb3s		Kb3	Kb5w		Kb5s		Kb5s
Location	Mid		Mid		Mid-change	GF		GF		GF change
	Mean	Min, max	Mean	Min, max	Mean	Mean	Min, max	Mean	Min, max	Mean
Salinity	34.85	34.81, 34.87	32.91	31.45, 34.50	*1.90*	34.80	34.50, 35.00	32.94	31.33, 34.37	*1.86*
Temperature (°C)	0.45	0.44, 0.47	4.68	3.73, 5.24	*−4.20*	−1.25	−1.50, −0.96	3.08	2.77, 3.27	*−4.33*
A_T (µmol kg^{-1})	2309	2307, 2314	2228	2160, 2299	*81*	2309	2300, 2333	2214	2172, 2284	*95*
C_T (µmol kg^{-1})	2160	2159, 2163	2027	1972, 2084	*133*	2158	2150, 2181	2008	1961, 2056	*150*
pH	8.117	8.102, 8.128	8.194	8.038, 8.270	*−0.077*	8.12	8.107, 8.128	8.24	8.158, 8.291	*−0.13*
fCO_2 (µatm)	321	313, 328	266	214, 382	*55*	321	313, 328	227	197, 282	*94*
Ω_c	2.63	2.57, 2.70	3.41	2.32, 4.01	*−0.78*	2.63	2.57, 2.70	3.47	2.94, 3.78	*−0.84*
Ω_a	1.65	1.62, 1.69	2.15	1.46, 2.53	*−0.49*	1.65	1.62, 1.69	2.18	1.85, 2.38	*−0.53*
NO_3 (mmol m^{-3})	9.95	9.6, 10.3	0.38	0.21, 0.83	*9.57*	7.07	6.58, 7.90	0.63	0.49, 0.80	*6.44*
PO_4 (mmol m^{-3})	0.78	0.69, 0.85	0.18	0.13, 0.26	*0.60*	0.53	0.49, 0.55	0.20	0.19, 0.21	*0.33*
Si (mmol m^{-3})	4.72	4.53, 4.95	1.30	1.04, 1.49	*3.42*	4.08	3.62, 4.42	1.40	1.17, 1.59	*2.68*
$A_{TS=35}$ (µmol kg^{-1})	2319	n/a	2238	n/a	*81*	2319	14	2224	n/a	*95*
$C_{TS=35}$ (µmol kg^{-1})	2169	n/a	2036	n/a	*134*	2168	13	2017	n/a	*151*
$pH_{S=35}$	8.123	n/a	8.259	n/a	*−0.136*	8.128		8.272	n/a	*−0.144*
$fCO_{2S=35}$ (µatm)	321	n/a	266	n/a	*56*	293		227	n/a	*66*
$\Omega_{cS=35}$	2.63	n/a	3.41	n/a	*−0.78*	2.64		3.47	n/a	*−0.83*
$\Omega_{aS=35}$	1.65	n/a	2.15	n/a	*−0.49*	1.66		2.18	n/a	*−0.52*
$NO_{3\ S=35}$ (mmol m^{-3})	10.00	n/a	0.38	n/a	*9.57*	7.21	0.55	0.64	n/a	*6.57*
$PO_{4S=35}$ (mmol m^{-3})	0.78	n/a	0.18	n/a	*0.60*	0.54	0.02	0.20	n/a	*0.34*
$Si_{S=35}$ (mmol m^{-3})	4.74	n/a	1.30	n/a	*3.42*	4.22	0.24	1.40	n/a	*2.82*

We show both original and salinity-normalized data to $S = 35$ for the chemical parameters (denoted in subscript $S = 35$). Aragonite and calcite saturation are denoted as Ω_a and Ω_c, respectively. Winter-to-summer difference (seasonal change) of the study parameters is shown as italics for the two stations. *n/a* not applicable

120 µatm occurred in 2014. The pH_T values were lowest in late winter in both years compared to the values in summer resulting in the largest seasonal increase in pH_T in 2014. Ω_a (and Ω_c) showed similar trends with the lowest values (1.6–1.7) occurring in late winter. The nutrients showed the opposite trend with the highest concentrations in late winter (max in April 2014) and the lowest in summer (Tables 3, 4). $[NO_3]_{S=35}$ in summer and winter surface waters was lower (by nearly 4 mmol m^{-3}) at the glacier front in 2013 compared to 2014 (Tables 3, 4). This implies that the winter-to-summer seasonal change in $[NO_3^-]$ was larger in 2014 than in 2013 at the glacier front.

Discussion

Water masses contain different concentrations of carbon and nutrients, and thus, their relative proportions will affect the carbonate chemistry in the Kongsfjorden. The warm and saline AW was more prominent in 2014, likely making the TAW warmer and more saline in this year compared to in 2013. The AW had the highest A_T values during both years, and because of low C_T, this resulted in some of the highest pH_T (>8.2) and Ω_a (>2) values in the studied area. In 2013, lower salinity and temperature suggest that the TAW had a larger influence from water transported by the coastal current (CC) relative to 2014. The Ω_a value in the TAW in 2013 was 0.4 lower than in 2014, suggesting that the CC decreased Ω_a and pH_T values. Few carbonate chemistry data are available from the East Spitsbergen Current (ESC), but data from Storfjorden and the southern Cape of Spitsbergen show that these waters have high C_T concentrations due to high fCO_2 levels. This high fCO_2 is caused by processes that are unique for sea ice-covered waters such as CO_2 production from the precipitation of $CaCO_3$ in brine during sea-ice formation (Rysgaard et al. 2007; Omar et al. 2005; Fransson et al. 2013). Chierici et al. (2014) reported high C_T values (2180–2200 µmol kg^{-1}) as a result of high CO_2 content near the southern cape of Spitsbergen. In this water, Ω_a was about 0.5 lower than the lowest Ω_a that was found in the TAW in

Table 4 Mean values and range shown as the minimum value (min) and the maximum value (max) of chemical and physical properties in winter (w) and summer (s) in the upper 30 m at two station locations in Kongsfjorden (mid, Kb3) and at the glacier front (GF, Kb5) in 2014

Year	2014		2014		2014	2014		2014		2014
Station	Kb3w		Kb3s		Kb3	Kb5w		Kb5s		Kb5
Location	Mid-w		Mid-s		Mid-change	GF-w		GF-s		GF change
	Mean	Min, max	Mean	Min, max	Mean	Mean	Min, max	Mean	Min, max	Mean
Salinity	35.14	34.13, 34.14	33.16	32.03, 34.52	*1.98*	34.84	34.80, 34.87	33.02	30.99, 34.65	*1.82*
Temperature (°C)	1.76	1.71, 1.82	5.14	4.23, 6.52	*−3.38*	−0.11	−0.17, −0.02	3.68	2.72, 5.02	*−3.79*
A_T (µmol kg^{-1})	2312.00	2311, 2314	2238	2166, 2303	*74*	2297	2296, 2299	2229	2156, 2302	*68*
C_T (µmol kg^{-1})	2156.00	2155, 2158	1999	1945, 2050	*157*	2149	2146, 2154	2010	1941, 2064	*139*
pH	8.109	8.109, 8.111	8.276	8.251, 8.297	*−0.17*	8.126	8.118, 8.135	8.261	8.226, 8.300	*−0.14*
fCO_2 (µatm)	329.00	328, 330	209	198, 228	*120*	312	305, 317	217	192, 240	*95*
Ω_c	2.73	2.72, 2.76	4.00	3.72, 4.18	*−1.27*	2.61	2.56, 2.66	3.68	3.42, 3.95	*−1.07*
Ω_a	1.72	1.71, 1.74	2.52	2.33, 2.64	*−0.80*	1.64	1.61, 1.67	2.31	2.15, 2.49	*−0.67*
NO_3 (mmol m^{-3})	11.35	10.60, 11.94	0.54	0.04, 1.25	*10.81*	11.53	11.18, 11.80	1.80	0.00, 2.70	*9.73*
PO_4 (mmol m^{-3})	0.72	0.68, 0.76	0.12	0.08, 0.16	*0.60*	0.72	0.69, 0.79	0.27	0.00, 0.32	*0.45*
Si (mmol m^{-3})	4.72	4.43, 4.96	1.52	1.15, 2.10	*3.20*	4.91	4.72, 5.07	2.02	0.00, 2.22	*2.89*
$A_{TS=35}$ (µmol kg^{-1})	2303	n/a	2230	n/a	*74*	2288	n/a	2221	n/a	*67*
$C_{TS=35}$ (µmol kg^{-1})	2157	n/a	1999	n/a	*157*	2141	n/a	2002	n/a	*139*
$pH_{S=35}$	8.117	n/a	8.322	n/a	*−0.205*	8.121	n/a	8.298	n/a	*−0.18*
$fCO_{2\ S=35}$ (µatm)	320	n/a	180	n/a	*120*	314	n/a	191	n/a	*123*
$\Omega_{cS=35}$	2.59	n/a	3.75	n/a	*−1.16*	2.60	n/a	3.57	n/a	*−0.97*
$\Omega_{aS=35}$	1.63	n/a	2.36	n/a	*−0.73*	1.63	n/a	2.24	n/a	*−0.61*
$NO_{3S=35}$ (mmol m^{-3})	11.31	n/a	0.38	n/a	*10.93*	11.49	n/a	1.79	n/a	*9.70*
$PO_{4S=35}$ (mmol m^{-3})	0.72	n/a	0.18	n/a	*0.54*	0.72	n/a	0.60	n/a	*0.12*
$Si_{S=35}$ (mmol m^{-3})	4.70	n/a	1.29	n/a	*3.41*	4.89	n/a	2.50	n/a	*2.39*

We show both original and salinity-normalized data to $S = 35$ for the chemical parameters (denoted in subscript $S = 35$). Aragonite and calcite saturation are denoted as Ω_a and Ω_c, respectively. Winter-to-summer difference (seasonal change) of the study parameters is shown as italics for the two stations. *n/a* not applicable

Kongsfjorden in 2013. Other carbonate chemistry data available from the Kongsfjorden were limited in both space and time but show similar spring/summer values to our data (EPOCA 2009 Svalbard benthic experiment. doi:10.1594/PANGAEA.745083; EPOCA Svalbard 2010 mesocosm experiment in Kongsfjorden, Svalbard, Norway. doi:10.1594/PANGAEA.769833; Riebesell et al. 2013).

The WSW had the lowest Ω_a value ($\sim$1.6), while the SSW had the highest Ω_a ($\sim$2.5 in 2014). The high Ω_a in summer was likely an effect of biological CO_2 uptake. Previous studies have shown that the increased Ω, because of biological CO_2 uptake during photosynthesis, counteracts decreases in Ω due to freshwater supply (Chierici and Fransson 2009; Chierici et al. 2011; Fransson et al. 2015). To investigate the net effect of these two processes, we inspected the influence of freshening due to addition of glacial water on the OA state at the glacier front, where the freshening signal is most pronounced. The effect of freshwater addition (calculated as fractions of freshwater) on Ω_a (and Ω_c) in Kongsfjorden was estimated by applying the formulation of the linear relation between Ω_a and freshwater fraction derived from a study in Tempelfjorden, another west Spitsbergen fjord (Fransson et al. 2015), which showed a 0.07 decrease in Ω_a for each 1 % increase in the freshwater fraction (Fig. 5). In the surface water at the glacier front, the change in freshwater fraction was 10–11 % in both years, resulting in Ω_a decrease by approximately −0.7. The effect on Ω_a due to biological carbon uptake was estimated using the nitrate concentration [NO_3^-] loss from late winter to summer (Tables 3, 4) and the empirically derived formulation by Chierici et al. (2011). In their study, Ω_a increased by 0.09 for each 1 mmol m^{-3} loss in salinity-normalized [NO_3^-]. The biological uptake of carbon increased Ω_a by 0.59 and 0.87 in 2013 and 2014, respectively. Based on these estimates, the increase of Ω_a due to biological carbon uptake (46–55 %) was of similar strength to the estimated decrease due to freshwater addition (45–54 %), although

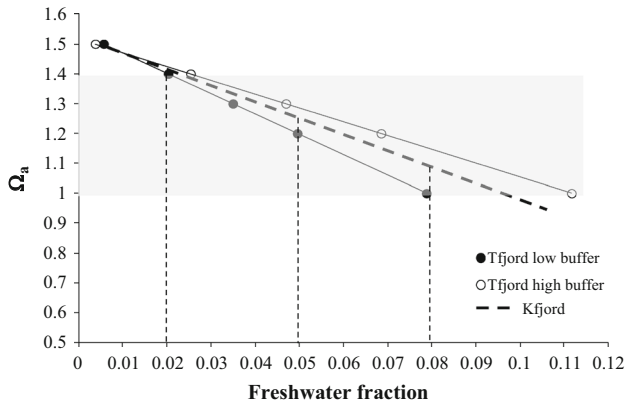

Fig. 5 Conceptual illustration of dilution scenarios at different total alkalinity content (A_T) in the freshwater source waters based on freshwater fractions (*x*-axis) versus aragonite saturation (*y*-axis, Ω_a) for Tempelfjorden at A_T of 526 µmol kg^{-1} (Tfjord low) and at the A_T of 1126 µmol kg^{-1} (Tfjord high). We added the projected change based on the A_T value of Kongsfjorden freshwater end member of 888 µmol kg^{-1} (Kfjord, *thick dashed line*), with the slope 0.07. *Vertical lines* emphasize the freshwater fraction at Ω_a of 1.4, 1.2 and 1, and *gray-shaded area* denotes the range of Ω_a where shell damage is initiated (1.4), to severe damage with net calcification (1.2) and undersaturation where calcification is strongly limited (< 1), as described in Bednaršek et al. (2012) The data from Tempelfjorden is adapted from Fransson et al. (2015)

the influence of the biological uptake showed larger interannual differences than the effect of freshwater. Our calculation for the influence of biological uptake only takes into account the CO_2 consumption from new production and does not consider consumption from regenerated or upwelled nutrients. Some studies of fjords show that upwelling of nutrients (and carbon) at the glacier front lead to high primary production in spring in the inner part of the fjord (e.g., Hodal et al. 2012; Hegseth and Tverberg 2013). However, in summer high loads of sediments in the inner bay cause aphotic conditions (at shallow depths), and the majority of the primary production takes place further out in the fjord (Piwosz et al. 2009). The direct warming effect on Ω_a was estimated by Chierici et al. (2011), where Ω_a increased by 0.009 per 1 °C increase. The relative effects on Ω_a showed that temperature had a minor effect of 4 % of the total Ω_a change due to combined temperature, freshening and biological carbon uptake.

Kongsfjorden has a similar physical marine environment as another west Spitsbergen fjord, Tempelfjorden, with the inflow of TAW and influence of glacial freshwater drainage from tide-water glaciers. In Tempelfjorden, Fransson et al. (2015) observed higher A_T in the freshwater source water in a warmer year (2012) with larger freshwater content in the fjord (1142 µmol kg^{-1}) compared with a colder winter (2013) when there was less freshwater content (526 µmol kg^{-1}). Higher A_T in freshwater is likely due to the supply of carbonate-rich glacial drainage water originating from calcite and dolomite minerals from the bedrock. Kongsfjorden is surrounded by the same type of bedrock containing calcite and dolomite (e.g., Dallmann et al. 2002), and the corresponding A_T in the freshwater source was about 890 µmol kg^{-1} ($A_T = 40.6 \times$ salinity + 890, $r^2 = 0.9$) in Kongsfjorden, similar to what was found in Tempelfjorden. Thus, buffering minerals (containing carbonate ions) in the glacial drainage water likely also affect A_T, the carbonate chemistry and OA state in Kongsfjorden.

We found the lowest Ω_a of 1.5 in the deep water of Kongsfjorden and Ω_a of 1.6 in the surface in late winter (April), which was similar to April values ($\Omega_a = 1.4$) in Tempelfjorden (Fransson et al. 2015). Such low Ω_a may be detrimental for the aragonite-forming organisms (Bednaršek and Ohman 2015). Laboratory experiments on *Limacina helicina* found reduced calcification and larval dissolution at $\Omega_a < 1$ (Comeau et al. 2009, 2010; Lischka et al. 2011; Lischka and Riebesell 2012), although it was also evident that calcification continued even at aragonite-undersaturated conditions (Comeau et al. 2010). Projected shoaling of the aragonite saturation horizon due to ocean acidification may change the depth of their diel vertical migration, as well as the overwintering depth, and could impact the length of time that these organisms are exposed to aragonite-undersaturated water (Comeau et al. 2010, 2011). This may have consequences for predatory pressure, especially on juveniles. Increased exposure to aragonite-undersaturated water may also have consequences for shell calcification and growth (Comeau et al. 2011). Studies from marine environments with large natural gradients in the carbonate chemistry confirmed the connection between low carbonate ion concentrations and damage (thinning and dissolution) of the aragonitic shells of *L. helicina* (Bednaršek and Ohman 2015), with severe dissolution occurring at Ω_a lower than 1.2–1.4 in the California Current upwelling system. In Kongsfjorden, the Ω_a values were lowest in the winter surface water (1.6) and increased to 2.5 in summer. Hence, in this fjord seasonally and spatially, *L. helicina* may already be living in Ω_a conditions that are detrimental.

Furthermore, synergistic effects of high winter temperatures (2–7 °C) and high fCO_2 (>650 µatm) in experiments have shown shell degradation of the *L. helicina,* in particular for overwintering juveniles (Lischka and Riebesell 2012). Since the life stage during winter is the most vulnerable stage of the *L. helicina*, in case of warmer winters, shell damage due to the contributing effect of increased temperature and increased fCO_2 could be critical for successful recruitment to the adult population. Thus, the winter season will likely be more critical for *L. helicina* than the summer, due to the lower Ω_a, the shallowing of the Ω_a horizon and less food availability (Lischka and Riebesell 2012). Any additional winter warming resulting in

increased supply and accumulation of freshwater from glacial water and river water supply would also affect Ω_a in fjords and increase the stress on *L. helicina*.

Interestingly, time-series sediment data in the eastern Fram Strait (west of Svalbard) showed that warming events resulted in a change of pteropod species from a prevalence of cold-water (Arctic)-associated *L. helicina* to the warm-water (Atlantic)-favoring *L. retroversa* (Bauerfeind et al. 2014). *Limacina retroversa* is probably introduced to Kongsfjorden with the AW and is not autochthonous (e.g., Hop et al. 2006). Consequently, the occurrence and abundance of *L. retroversa* could be used as an indicator for the warm AW in Kongsfjorden and adjacent seas (Lischka and Riebesell 2012). The change from Arctic species to the Atlantic species in parts of the fjord may have consequences for the carbon cycling and export to deeper water layers. Further investigation is required to assess whether these species have different sensitivities to changes in carbonate chemistry (and consequently future OA), which could impact how these populations survive in Kongsfjorden.

Previous studies show that the AW contains high amounts of anthropogenic CO_2 (e.g., Sabine et al. 2004), due to efficient anthropogenic CO_2 uptake during cooling as the AW is transported northward along the Norwegian Coast. Olsen et al. (2006) estimated the rate of fCO_2 increase due to anthropogenic CO_2 uptake to be about 1 µatm year^{-1} in the WSC and on the west Spitsbergen shelf. Assuming no change in A_T, salinity and temperature, this corresponds to a decadal decrease of 0.04 in Ω_a. This means that if only anthropogenic CO_2 uptake is taken into account, it would take about 50 years to reach the highest threshold level for damage of the shell reported to occur at Ω_a of 1.4 from the current winter surface minimum of 1.6 (and deep minimum of 1.5). However, these threshold levels are uncertain since they are based on different *L. helicina* populations, and do not consider specific ecology of pteropods (e.g., diel and seasonal migrations of pteropods and latitude could be influential). Anthropogenic CO_2 uptake in combination with other climate drivers such as increased freshwater addition and warming will likely accelerate ocean acidification and result in detrimental conditions for calcifying organisms. However, compensatory mechanisms, such as adaptation, changes in energy balance, phenotypic plasticity and genetic selection at the population level, could, to some extent, reduce the negative effects on the calcifying organisms and need to be considered (e.g., Thor and Dupont 2015).

We present a conceptual illustration (Fig. 6) of various effects on Ω_a in Kongsfjorden in winter and summer, with two scenarios: (1) colder and less saline (Arctic regime)

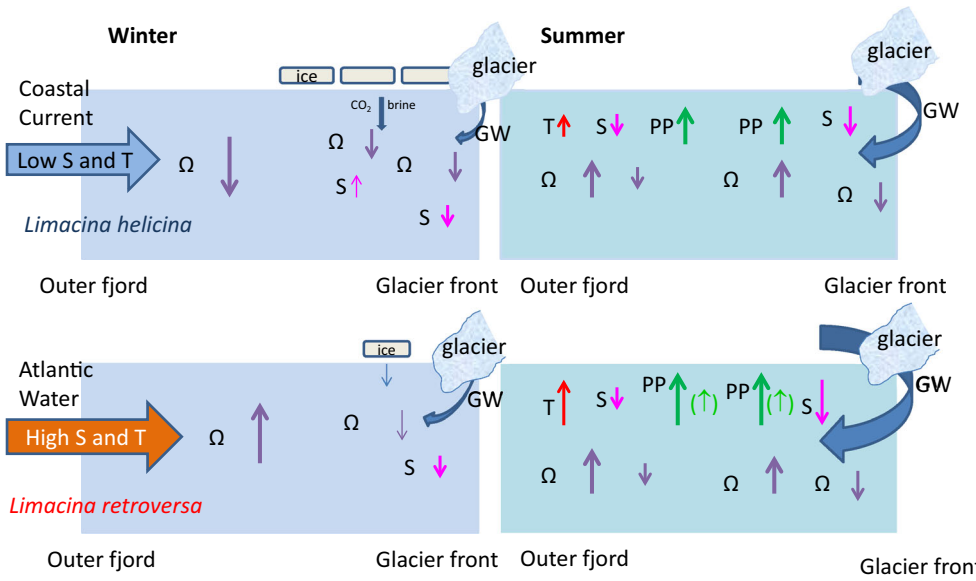

Fig. 6 Conceptual model of different effects such as salinity change due to ice formation and ice melt (*S*), temperature change (*T*), primary production (PP) and glacial water inflow (GW) on $CaCO_3$ saturation (Ω) in the upper 30 m in winter and summer in Kongsfjorden during two scenarios; (1) inflow of predominating coastal current water (CC, *upper display*) and (2) inflow of predominating Atlantic water (AW, *lower display*). Both scenarios include inflow of glacial water (GW). The magnitude of the resulting change in Ω from the processes is depicted using size and direction of arrows. *Small arrows* depict a relatively small change, and *large arrows* show a relatively larger effect on Ω. The *smaller arrows* of PP in parenthesis mean that during late summer, strong stratification may introduce nutrient limitation for PP. During late summer, PP declines because of light limitation due to sediment supply from glacial water, but also because of community changes and sinking down of the plankton biomass (deep chlorophyll maximum). CC is colder and less saline (with lower Ω) than AW, which is warmer and more saline (with higher Ω). In the colder regime, *Limacina helicina* is the dominant species of pteropod species, but is replaced by *Limacina retroversa* in the warm regime

and (2) warmer and more saline (Atlantic regime). In the colder scenario, *L. helicina* will most likely be the predominant species and *L. retroversa* in the warmer scenario (Bauerfeind et al. 2014). Based on our study, the TAW in Kongsfjorden is either influenced by the inflow of a larger component of colder and less saline (and lower Ω_a) water transported by the coastal current (CC) or influenced by the inflow of warmer and more saline Atlantic water (AW; higher Ω_a). Landfast sea ice forms in the fjords during winter, when the conditions are sufficiently cold, resulting in rejection of CO_2-rich brine (which decreases Ω_a) from the ice to underlying water. Freshwater supply also decreases Ω_a, and this effect may be greater in a warmer scenario due to higher glacial water (GW) discharge. In spring and summer, the surface water becomes stratified and photosynthesis (primary production) initiates the biological CO_2 uptake, which consequently increased Ω_a. In the warmer scenario (AW scenario), more meltwater (decreased Ω_a) will likely create stronger stratification, causing a larger, earlier bloom in phytoplankton, resulting in a larger increase in Ω_a. However, early blooms may become nutrient limited in stratified water masses or light limited in the inner basin because of suspended sediments. In Kongsfjorden, increased meltwater runoff from the glaciers due to enhanced inflow of warm AW entering the WSC is expected in the future (Piquet et al. 2014). This freshwater may result in decreased Ω_a, potentially causing multistress impacts on calcifying organisms such as *L. helicina*, by generating physiological stress due to lower salinity, higher temperatures and increasing the risk of dissolution and thinning of their aragonitic shells. The thinner (lighter) shells will consequently cause less carbon export out of the mixed layer to the deep ocean, as suggested by Bednaršek et al. (2014). Moreover, increased advection of CO_2-rich waters from east of Svalbard and Storfjorden transported in the CC will contribute to further decreased Ω_a in the Kongsfjorden, the west Spitsbergen shelf and further north into the Arctic Ocean (Fig. 6). Biological carbon uptake during summer may increase due to increased AW in the outer parts of the fjord, increasing Ω_a. However, at the inner parts of the fjord, Ω_a may decrease in summer due to enhanced freshening and less biological carbon uptake as a result of nutrient and light limitations. For a complete understanding of the effect of multiple stressors on the marine ecosystem, we suggest a combination of modeling efforts and integrated observational programs with sampling of physical and chemical parameters and biological collection of particularly sensitive species across large natural gradients.

Acknowledgments This is a project within the flagship research program "Ocean acidification and ecosystem effects in Northern waters" at the Fram Centre, and MOSJ (Monitoring of Svalbard), and we thank the Ministry of Climate and Environment and the Ministry of Trade, Industry and Fisheries, Norway, for financial support. Data will be stored at the Norwegian Polar Institute data archive and be available within 1 year after publication. Metadata will also be available at RiS portal at www.researchinsvalbard.no within 1 year after publication; until then contact the corresponding author. We gratefully thank the captain and crew on RV *Lance* for valuable support and assistance and all students or researchers who helped with water sampling. We gratefully thank Malcolm Woodward for the nutrient analyses (April 2014). We are also grateful for the support, boat logistics and safety training at the Norwegian Polar Institute logistics in Ny-Ålesund. We thank Michael Greenacre and three anonymous reviewers for valuable comments for improving the manuscript.

References

Accornero A, Manno C, Esposito F, Gambi MC (2003) The vertical flux of particulate matter in the polynya of Terra Nova Bay, Part II, Biological components. Antarct Sci 15:175–188

Apollonio S (1973) Glaciers and nutrients in Arctic seas. Science 180:491–493

Bauerfeind E, Nöthig E-M, Pauls B, Kraft A, Beszczynska-Möller A (2014) Variability in pteropod sedimentation and corresponding aragonite flux at the Arctic deep-sea long-term observatory HAUSGARTEN in the eastern Fram Strait from 2000 to 2009. J Mar Syst 132:95–105. doi:10.1016/j.jmarsys.2013.12.006

Bednaršek N, Ohman MD (2015) Changes in pteropod distributions and shell dissolution across a frontal system in the California Current System. Mar Ecol Prog Ser 523:93–103. doi:10.3354/meps11199

Bednaršek N, Tarling GA, Bakker DCE, Fielding S, Jones EM, Venables HJ, Ward P, Kuzirian A, Lézé B, Feely RA, Murphy EJ (2012) Extensive dissolution of live pteropods in the Southern Ocean. Nat Geosci. doi:10.1038/NGEO1635

Bednaršek N, Tarling GA, Bakker DCE, Fielding S, Feely RA (2014) Dissolution dominating calcification process in polar pteropods close to the point of aragonite undersaturation. PLoS ONE 9(10):e109183. doi:10.1371/journal.pone.0109183

Bendschneider K, Robinson RI (1952) A new spectrophotometric method for the determination of nitrite in seawater. J Mar Res 2:87–96

Brewer PG, Riley JP (1965) The automatic determination of nitrate in sea water. Deep Sea Res 12:765–772

Chierici M, Fransson A (2009) $CaCO_3$ saturation in the surface water of the Arctic Ocean: undersaturation in freshwater influenced shelves. Biogeosciences 6:2421–2432

Chierici M, Fransson A, Lansard B, Miller LA, Mucci A, Shadwick E, Thomas H, Tremblay J-E, Papakyriakou T (2011) The impact of biogeochemical processes and environmental factors on the calcium carbonate saturation state in the Circumpolar Flaw Lead in the Amundsen Gulf, Arctic Ocean. J Geophys Res Oceans 116:C00G09. doi:10.1029/2011JC007184

Chierici M, Skjelvan I, Bellerby R, Norli M, Lunde Fonnes L, Lødemel Hodal H, Børsheim KY, Lauvset KS, Johannessen T, Sørensen K, Yakushev E (2014) Overvåking av havforsuring i norske farvann, Miljødirektoratet, Report TA218-2014

Comeau S, Gorsky G, Jeffree R, Teyssié J-L, Gattuso J-P (2009) Impact of ocean acidification on a key Arctic pelagic mollusk (*Limacina helicina*). Biogeosciences 6:1877–1882

Comeau S, Jeffree R, Teyssié J-L, Gattuso J-P (2010) Response of the Arctic pteropod *Limacina helicina* to projected future environmental conditions. PLoS ONE 5:e11362. doi:10.1371/journal.pone.0011362

Comeau S, Gattuso J-P, Nisumaa A-M, Orr J (2011) Impact of aragonite saturation state changes on migratory pteropods. Proc R Soc Ser B 279:732–738. doi:10.1098/rspb.2011.0910

Cottier FR, Tverberg V, Inall ME, Svendsen H, Nilsen F, Griffiths C (2005) Water mass modification in an Arctic fjord through cross-shelf exchange: the seasonal hydrography of Kongsfjorden, Svalbard. J Geophys Res Oceans 110:C12005

Cottier FR, Nilsen F, Inall ME, Gerland S, Tverberg V, Svendsen H (2007) Wintertime warming of an Arctic shelf in response to large-scale atmospheric circulation. Geophys Res Lett 34:L10607

Dallmann WK, Ohta Y, Elvevold S, Blomeier D (2002) Bedrock map of Svalbard and Jan Mayen, Norsk Polarinstitutt Temakart 33. Norwegian Polar Institute, Tromsø

Dalpadado P, Hop H, Rønning J, Pavlov V, Sperfeld E, Buchholz F, Rey A, Wold A (2016) Distribution and abundance of euphausiids and pelagic amphipods in Kongsfjorden, Isfjorden and Rijpfjorden (Svalbard) and changes in their relative importance as key prey in a warming marine ecosystem. Polar Biol. doi:10.1007/s00300-015-1874-x

Dickson AG (1990) Standard potential of the (AgCl(s) + 1/2H_2 (g) = Ag(s) + HCl(aq)) cell and the dissociation constant of bisulfate ion in synthetic sea water from 273.15 to 318.15 K. J Chem Thermodyn 22:113–127

Dickson AG, Millero FJ (1987) A comparison of the equilibrium constants for the dissociation of carbonic acid in seawater media. Deep Sea Res 34:1733–1743

Dickson AG, Sabine CL, Christian JR (2007) Guide to best practices for ocean CO_2 measurements. PICES Special Publication 3, 191 pp

Fabry VJ, Seibel BA, Feely RA, Orr JC (2008) Impacts of ocean acidification on marine fauna and ecosystem processes. ICES J Mar Sci 65:414–432. doi:10.1093/icesjms/fsn048

Falk-Petersen S, Sargent JR, Kwasniewski S, Gulliksen B, Millar R-M (2001) Lipids and fatty acids in *Clione limacina* and *Limacina helicina* in Svalbard waters and the Arctic Ocean: trophic implications. Polar Biol 24:163–170

Findlay HS, Wood HL, Kendall MA, Spicer JI, Twitchett R, Widdicombe S (2011) Comparing the impact of high CO_2 on calcium carbonate structures in difference marine organisms. Mar Biol Res 7:565–575

Fransson A, Chierici M, Miller LA, Carnat G, Thomas H, Shadwick E, Pineault S, Papakyriakou TM (2013) Impact of sea ice processes on the carbonate system and ocean acidification state at the ice-water interface of the Amundsen Gulf, Arctic Ocean. J Geophys Res Oceans 118:1–23. doi:10.1002/2013JC009164

Fransson A, Chierici M, Nomura D, Granskog MA, Kristiansen S, Martma T, Nehrke G (2015) Effect of glacial drainage water on the CO_2 system and ocean acidification state in an Arctic tidewater-glacier fjord during two contrasting years. J Geophys Res Oceans. doi:10.1002/2014JC010320

Gannefors C, Böer M, Kattner G, Graeve M, Eiane K, Gulliksen B, Hop H, Falck-Petersen S (2005) The Arctic butterfly *Limacina helicina*: lipids and life strategy. Mar Biol 147:169–177. doi:10.1007/s00227-004-1544-y

Gerland S, Renner A (2007) Sea ice mass balance monitoring in an Arctic fjord. Ann Glaciol 46:435–442

Gilmer RW, Harbison GR (1991) Diet of *Limacina helicina* (Gastropoda: Thecosomata) in Arctic waters in midsummer. Mar Ecol Prog Ser 77:125–134

Grasshoff H (1976) Methods of sea water analysis. Verlag Chemie, Basel

Grasshoff K, Kremling K, Ehrhardt M (2009) Methods of seawater analysis, 3rd edn. Wiley, New York

Hegseth EN, Tverberg V (2013) Effect of Atlantic water inflow on timing of the phytoplankton spring bloom in a high Arctic fjord (Kongsfjorden, Svalbard). J Mar Syst 113–114:94–105

Hodal H, Falk-Petersen S, Hop H, Kristiansen S, Reigstad M (2012) Spring bloom dynamics in Kongsfjorden, Svalbard: nutrients phytoplankton, protozoans and primary production. Polar Biol 35:191–203

Hop H, Pearson T, Hegseth EN, Kovacs KM, Wiencke C, Kwasniewski C, Eiane S, Mehlum F, Gullriksen B et al (2002) The marine ecosystem of Kongsfjorden, Svalbard. Polar Res 21:167–208

Hop H, Falk-Petersen S, Svendsen H, Kwasniewski S, Pavlov V, Pavlov O, Søreide JE (2006) Physical and biological characteristics of the pelagic system across Fram Strait to Kongsfjorden. Progr Oceanogr 71:182–231

Hunt BPV, Pakhomov EA, Hosie GW, Siegel V, Ward P, Bernard K (2008) Pteropods in southern ocean ecosystems. Prog Oceanogr 78:193–221

Keck A, Wiktor J, Hapter R, Nilsen R (1999) Plankton assemblages related to physical gradients in an Arctic, glacier-fed fjord in summer. ICES J Mar Sci 56:203–214

Kirkwood DS (1989) Simultaneous determination of selected nutrients in sea water. Report CM 1989/C:29, Copenhagen: International Council for the Exploration of the Seas

Kobayashi HA (1974) Growth cycle and related vertical distribution of the thecosomatous pteropod *Spiratella* ("*Limacina*") *helicina* in the central Arctic Ocean. Mar Biol 26:295–301. doi:10.1007/BF00391513

Kurihara H (2008) Effects of CO_2-driven ocean acidification on the early developmental stages of invertebrates. Mar Ecol Prog Ser 373:275–284. doi:10.3354/meps07802

Lischka S, Riebesell U (2012) Synergistic effects of ocean acidification and warming on overwintering pteropods in the Arctic. Glob Change Biol 18:3517–3528. doi:10.1111/geb.12020

Lischka S, Büdenbender J, Boxhammer T, Riebesell U (2011) Impact of ocean acidification and elevated temperatures on early juveniles of the polar shelled pteropod *Limacina helicina*: mortality, shell degradation, and shell growth. Biogeosciences 8:919–932. doi:10.5194/bg-919-2011

Lydersen C, Assmy P, Falk-Petersen S, Kohler J, Kovacs KM, Reigstad M, Steen H, Strøm H, Sundfjord A, Varpe Ø, Walczowski W, Weslawski JM, Zajaczkowski M (2014) The importance of tidewater glaciers for marine mammals and seabirds in Svalbard, Norway. J Mar Syst 129:452–471

Manno C, Tirelli V, Accornero A, Umani SF (2010) Importance of the contribution of *Limacina helicina* faecal pellets to the carbon pump in Terra Nova Bay (Antarctica). J Plankton Res 32:145–152

Mehrbach C, Culberson CH, Hawley JE, Pytkowicz RM (1973) Measurement of the apparent dissociation constants of carbonic acid in seawater at atmospheric pressure. Limnol Oceanogr 18:897–907. doi:10.4319/lo.1973.18.6.0897

Mucci A (1983) The solubility of calcite and aragonite in seawater at various salinities, temperatures and at one atmosphere pressure. Am J Sci 283:781–799

Olsen A, Omar AM, Bellerby RGJ, Johannessen T, Ninnemann U, Brown KR, Olsson KA, Olafsson J, Nondal G, Kivimäe C, Kringstad S, Neill C, Olafsdottir S (2006) Magnitude and origin of the anthropogenic CO_2 increase and ^{13}C Suess effect in the Nordic seas since 1981. Global Biogeochem Cycles 20:GB3027. doi:10.1029/2005GB002669

Omar A, Johannessen T, Bellerby R, Olsen A, Anderson LG, Kivimäe C (2005) Sea-ice and brine formation in Storfjorden: implications for the Arctic wintertime air-sea CO_2 flux. In: Drange H (ed) The Nordic seas - an integrated perspective. American Geophysical Union (AGU), pp 177–188

Pierrot D, Lewis E, Wallace DWR (2006) MS excel program developed for CO_2 system calculations, ORNL/CDIAC-105. Carbon Dioxide Information Analysis Center, Oak Ridge National Laboratory, U.S. Department of Energy, Oak Ridge

Piquet AM-T, van de Poll WH, Visser RJW, Wiencke C, Bolhuis H, Buma AGJ (2014) Springtime phytoplankton dynamics in Arctic Krossfjorden and Kongsfjorden (Spitsbergen) as a function of glacier proximity. Biogeosciences 11:2263–2279. doi:10.5194/bg-11-2263-2014

Piwosz K, Walkusz W, Hapter R, Wieczorek P, Hop H, Wiktor J (2009) Comparison of productivity and phytoplankton in warm (Kongsfjorden) and a cold (Hornsund) Spitsbergen fjord in mid-summer 2002. Polar Biol 32:549–559

Redfield A, Ketchum BH, Richards FA (1963) The influence of organisms on the composition of sea water. In: Hill NM (ed) The Sea, vol 2. Interscience, New York, pp 26–77

Riebesell U, Gattuso J-P, Thingstad TF, Middelburg JJ (2013) Arctic ocean acidification: pelagic ecosystem and biogeochemical responses during a mesocosm study. Biogeosciences 10:5619–5626. doi:10.5194/bg-10-5619-2013

Ries JB (2012) Oceanography: a sea butterfly flaps its wings. Nat Geosci 5:845–846

Rysgaard S, Glud RN, Sejr MK, Bendtsen J, Christensen PB (2007) Inorganic carbon transport during sea ice growth and decay: a carbon pump in polar seas. J Geophys Res 112:C03016. doi:10.1029/2006JC003572

Sabine CL, Feely RA, Gruber N, Key RM, Lee K, Bullister JL, Wanninkhof R, Wong CS, Wallace DWR, Tilbrook B, Millero FJ, Peng T-H, Kozyr A, Ono T, Rios AF (2004) The oceanic sink for anthropogenic CO_2. Science 305:367–371. doi:10.1126/science.1097403

Sejr MK, Krause-Jensen D, Rysgaard S, Sørensen LL, Christensen PB, Glud RN (2011) Air–sea flux of CO_2 in arctic coastal waters influenced by glacial melt water and sea ice. Tellus 63B:815–822

Shadwick EH, Thomas H, Chierici M, Fransson A et al (2011) Seasonal variability of the inorganic carbon system in the Amundsen Gulf region of the southeastern Beaufort Sea. Limnol Oceanogr 56:303–322. doi:10.4319/lo.2011.56.1.0303

Svendsen H, Beszczynska-Møller A, Hagen JO, Lefauconnier B, Tverberg V et al (2002) The physical environment of Kongsfjorden–Krossfjorden, an Arctic fjord system in Svalbard. Polar Res 21:133–166

Thor P, Dupont S (2015) Transgenerational effects alleviate severe fecundity loss during ocean acidification in an ubiquitous planktonic copepod. Glob Change Biol 21:2261–2271

Tréguer P, Legendre L, Rivkin RT, Raueneau O, Dittert N (2013) Water column biogeochemistry below the euphotic zone. In: Fasham MJR (ed) Ocean biogeochemistry: the role of the ocean carbon cycle in global change, global change—the IGBP series (closed), pp 145–156. doi:10.1007/978-3-642-55844-3.7.2003

Walczowski W (2013) Frontal structures in the West Spitsbergen Current margins. Ocean Sci 9:957–975. doi:10.5194/os-9-957-2013

Woodward EMS, Rees AP (2001) Nutrient distributions in an anticyclonic eddy in the northeast Atlantic Ocean, with reference to nanomolar ammonium concentrations. Deep Sea Res Part II 48:775–793

Yamamoto-Kawai M, McLaughlin FA, Carmack ECS, Nishino S, Shimada K (2009) Aragonite undersaturation in the Arctic Ocean: effects of ocean acidification and sea ice melt. Science 326:1098–1100. doi:10.1126/science.1174190

Zhang J-Z, Chi J (2002) Automated analysis of nanomolar concentrations of phosphate in natural waters with liquid waveguide. Environ Sci Techol 36:1048–1053